



Competitive antagonism of insect GABA receptors by iminopyridazine derivatives of GABA

Mohammad Mostafizur Rahman^a, Yuki Akiyoshi^b, Shogo Furutani^c, Kazuhiko Matsuda^c, Kenjiro Furuta^b, Izumi Ikeda^{a,b}, Yoshihisa Ozoe^{a,b,*}

^a Division of Bioscience and Biotechnology, United Graduate School of Agricultural Sciences, Tottori University, Tottori 680-8553, Japan

^b Department of Life Science and Biotechnology, Faculty of Life and Environmental Science, Shimane University, Matsue, Shimane 690-8504, Japan

^c Department of Applied Biological Chemistry, Faculty of Agriculture, Kinki University, 3327-204 Nakamachi, Nara 631-8505, Japan

ARTICLE INFO

Article history:

Received 24 April 2012

Revised 23 July 2012

Accepted 23 July 2012

Available online 8 August 2012

Keywords:

Iminopyridazine

Competitive antagonism

GABA receptor

GABA-gated chloride channel

Insect

Insecticide

ABSTRACT

A series of 4-(6-imino-3-aryl/heteroarylpyridazin-1-yl)butanoic acids were synthesized and examined for antagonism of GABA receptors from three insect species. When tested against small brown planthopper GABA receptors, the 3,4-methylenedioxyphenyl and the 2-naphthyl analogues showed complete inhibition of GABA-induced fluorescence changes at 100 μM in assays using a membrane potential probe. Against common cutworm GABA receptors, these analogues displayed approximately 86% and complete inhibition of GABA-induced fluorescence changes at 100 μM , respectively. The 4-biphenyl and 4-phenoxyphenyl analogues showed moderate inhibition at 10 μM in these receptors, although the inhibition at 100 μM was not complete. Against American cockroach GABA receptors, the 4-biphenyl analogue exhibited the greatest inhibition (approximately 92%) of GABA-induced currents, when tested at 500 μM using a patch-clamp technique. The second most active analogue was the 2-naphthyl analogue with approximately 85% inhibition. The 3-thienyl analogue demonstrated competitive inhibition of cockroach GABA receptors. Homology modeling and ligand docking studies predicted that hydrophobic 3-substituents could interact with an accessory binding site at the orthosteric binding site.

© 2012 Elsevier Ltd. All rights reserved.

1. Introduction

γ -Aminobutyric acid (GABA) is the major inhibitory neurotransmitter in the nervous system of animals. GABA released into the synapse functions by binding to two types of membrane proteins: ionotropic and metabotropic receptors.^{1,2} The ionotropic GABA receptor belongs to the Cys-loop receptor family and mediates fast synaptic inhibition.^{1,3} The receptors of this family are ligand-gated ion channels that are formed by five subunits. There are two types of ionotropic receptors in mammals: hetero-pentameric GABA_A receptors, which are composed of α 1-6, β 1-3, γ 1-3, δ , ϵ , θ , and π subunits, and homo-pentameric GABA_C receptors, which comprise ρ 1-3 subunits.⁴ GABA_A receptors with an α 1- β 2- γ 2 combination are the most abundant subtype in the brain.⁴ When GABA or an agonist binds to the orthosteric site in the α - β subunit interface of the extracellular domain of GABA_A receptors, the integral channel rapidly opens to increase the membrane conductance of chlo-

ride ions, thereby suppressing the generation of action potentials. GABA_A receptors are also targets for drugs such as benzodiazepines, barbiturates, and anesthetics.⁵ In addition to agonists and drugs, two known types of antagonists exist for the Cys-loop receptor: competitive antagonists, which bind to the same site as agonists do, and noncompetitive antagonists, which bind to an allosteric binding site in the channel domain.^{5,6} Both types of antagonists stabilize the closed conformation of the channels and block membrane conductance.

GABA receptors are widely distributed in both insect and mammalian nerve tissues. Insect GABA receptors exist not only in the central nervous system but also in the peripheral nervous system.⁷ Inhibitory GABA receptor genes have been cloned from several insect species to date. In *Drosophila*, molecular cloning and functional expression of excitatory and metabotropic types of receptors have also been reported.⁸⁻¹⁰ Insect inhibitory GABA receptors can be expressed as homo-pentamers, the subunits of which are encoded by the single gene *rdl*, but four subunit variants are generated by alternative splicing of the exons 3 and 6 of *rdl*.¹¹ Homo-oligomeric RDL receptors share distinctive characteristics with native GABA receptors. Although insect GABA receptors are structurally similar to mammalian GABA receptors, these two receptors have different pharmacological characteristics, allowing GABA receptors to serve

Abbreviations: AC, American cockroach; CC, common cutworm; FLIPR, fluorometric imaging plate reader; FMP, FLIPR membrane potential; GABA, γ -aminobutyric acid; SBP, small brown planthopper.

* Corresponding author. Tel./fax: +81 852 32 6573.

E-mail address: ozoe-y@life.shimane-u.ac.jp (Y. Ozoe).

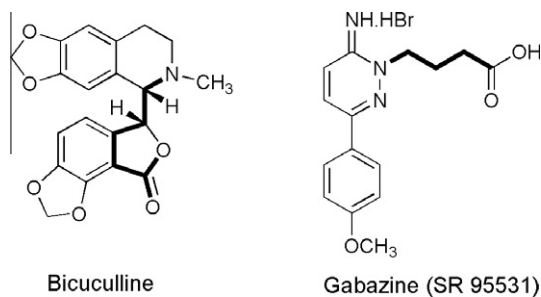


Figure 1. Structures of bicuculline and gabazine (SR 95531). Bold lines show the GABA structural units.

as important targets for insecticides and parasiticides.^{11,12} For example, the noncompetitive antagonist fipronil is used as an insecticide.¹³ In contrast, no competitive antagonist has been exploited in this respect. Although bicuculline and gabazine (SR 95531) (Fig. 1) are well known as competitive antagonists for mammalian GABA_A receptors,^{14,15} no potent competitive antagonist for insect GABA receptors is known. While bicuculline is inactive for insect GABA receptors, gabazine was found to have moderate antagonist activity against insect GABA receptors.^{16–18}

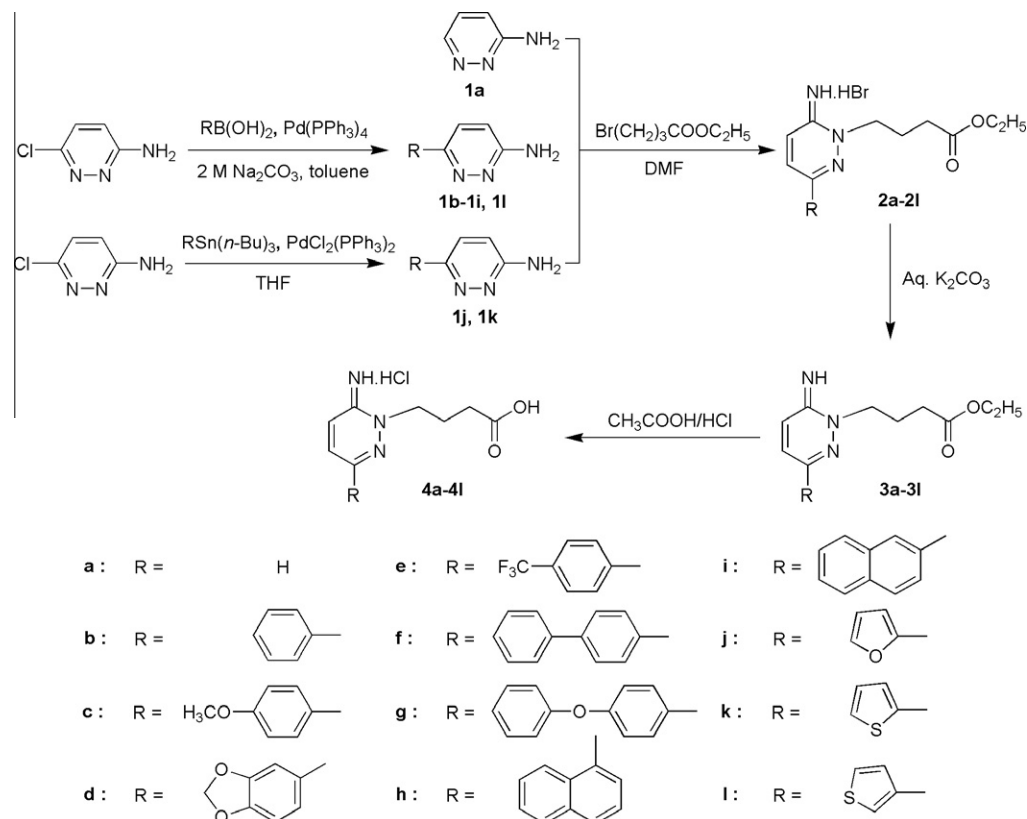
In this study, we examined whether the antagonist activity of gabazine against insect GABA receptors is increased by changing the 3-substituent on the pyridazine ring. Here, we used GABA receptors cloned from two insect species, small brown planthoppers (SBPs, *Laodelphax striatella* [striatellus] (Fallén)) and common cutworms (CCs, *Spodoptera litura* (Fabricius)), which cause serious damage on crops, and native GABA receptors expressed in the abdominal ganglion neurons of American cockroaches (ACs, *Periplaneta americana* (Linnaeus)), a noxious insect species. With GABA

receptors from three insect species, we seek to find species differences in the receptors to utilize the information for future discovery and the development of chemicals for insect pest control.

2. Results and discussion

2.1. Chemistry

In this study, we synthesized a series of iminopyridazine derivatives of GABA, which consisted of 4-(6-iminopyridazin-1-yl)butanoic acids, by modifying the 3-position of the pyridazine ring (Scheme 1). Wermuth et al. first described a seven-step synthetic approach including pyridazinone intermediates for **4b**, **4c** (gabazine, SR 95531), **4k**, and **4l**.¹⁹ The synthesis of **4d** was reported by Melikian et al.,²⁰ which also required seven synthetic steps. Recently, Gavande et al. described a four-step synthesis procedure for **4c** under microwave irradiation conditions starting with 3,6-dichloropyridazine.²¹ Here, we have demonstrated an efficient three-step synthesis of eleven 3-aryl/heteroaryl analogues starting with 3-amino-6-chloropyridazine and a two-step synthesis of a 3-unsubstituted analogue from 3-aminopyridazine (Scheme 1). The first intermediates of nine analogues (**1b–1i**, **1l**) were synthesized in 19–78% yield using the Suzuki–Miyaura cross-coupling reaction where aryl/heteroarylboronic acid was coupled with 3-amino-6-chloropyridazine in presence of a palladium catalyst and a base such as sodium carbonate. The first intermediates of two analogues (**1j**, **1k**) were synthesized in 73% and 75% yield, respectively, using the Stille cross-coupling reaction between tributyl(heteroaryl)tin and 3-amino-6-chloropyridazine in the presence of a palladium catalyst. The N(2)-alkylated compounds **2a–2l** in the second step were synthesized in 11–74% yield by the reactions between **1a–1l** and ethyl 4-bromobutanoate. Free base esters of the alkylated compounds **3a–3l** were prepared in 77–93% yield from **2a–2l** using



Scheme 1. Synthesis of 4-(6-iminopyridazin-1-yl)butanoic acid hydrochlorides.

K_2CO_3 . Hydrolysis of the free base esters was carried out in acetic acid and hydrochloric acid at 100 °C in 63–97% yield to give the target compounds **4a–4l**.

2.2. Antagonism of SBP and CC GABA receptors

The application of GABA to membrane potential probe-loaded cells expressing GABA receptors increases fluorescence, which is detected by fluorometric imaging plate reader (FLIPR) membrane potential (FMP) assays.^{22,23} Antagonist activity can be assessed from a fluorescence reduction induced by a co-applied compound. When tested at 100 μ M, an analogue with no substituent at the 3-position of the pyridazine ring (**4a**) showed no or little antagonism against SBP and CC GABA receptors (Figs. 2 and 3). The introduction of a phenyl group into the 3-position of **4a** led to **4b** with weak activity. The inclusion of a methoxy group at the 4-position of the phenyl group of **4b** to give gabazine (**4c**) resulted in a 2.7- and 3.3-fold increase in the inhibition of GABA-induced fluorescence increases in SBP and CC receptors, respectively. The replacement of the 4-methoxy group of **4c** with a 3,4-methylenedioxy group, yielding **4d**, led to complete inhibition and 85.8% inhibition in SBP and CC GABA receptors, respectively. The antagonist activity of the 4-trifluoromethylphenyl analogue (**4e**) was comparable to that of the 4-methoxyphenyl analogue (**4c**) in SBP receptors but **4e** showed lower activity than **4c** in CC receptors. The 4-biphenyl analogue (**4f**) did not exceed **4c** in terms of antagonist activity at 100 μ M in SBP receptors and showed inhibition comparable to that of **4c** in CC receptors, but it is notable that **4f** showed a moderate activity even at 10 μ M in both receptors. The 4-phenoxyphenyl analogue (**4g**) was inferior to the 4-biphenyl analogue (**4f**) in SBP receptors whereas they are comparable in CC receptors. While the 1-naphthyl analogue (**4h**) was only moderately active or inactive at 100 μ M in SBP and CC receptors, the 2-naphthyl analogue (**4i**) completely inhibited GABA-induced responses at 100 μ M in both receptors and showed approximately 41% and 29% inhibition at 10 μ M in SBP and CC receptors, respectively. Thus, the 2-naphthyl substitution is preferable to the 1-naphthyl substitution; the naphthyl ring of **4h** may provide a significant amount of steric hindrance for binding to the site. The 2-naphthyl analogue (**4i**) per se showed agonist-like activity (i.e., caused an increase in fluorescence) at 100 μ M, and co-application of GABA failed to induce an increase in fluorescence (data not shown). The substitution of the

3-substituent with 2-furyl and 2-thienyl groups to yield **4j** and **4k** nearly eliminated the antagonist activity. Substitution with a 3-thienyl group produced an analogue (**4l**) with moderate activity in both receptors.

Finally, we examined whether competitive GABA receptor antagonism leads to insecticidal activity against SBP and CC larvae. While showing significant antagonism against the GABA receptors of these insects, the 4-biphenyl analogue (**4f**) did not exert insecticidal effects (data not shown), indicating that higher in vitro potency is necessary for insecticidal activity.

2.3. Antagonism of AC GABA receptors

The antagonism of native AC GABA receptors by the synthesized analogues was measured using the whole-cell patch-clamp technique. Figure 4A shows that GABA-induced currents are inhibited by the 4-biphenyl analogue (**4f**). After confirmation of the constant amplitude of GABA-induced currents, the neurons were perfused with an external solution containing 500 μ M **4f**. During the perfusion, GABA was repeatedly applied five times. This analogue attenuated the currents progressively, and a maximum inhibition of 92.0% was attained after the third application. The other analogues were also tested in this fashion.

The phenyl (**4b**) and 4-methoxyphenyl (**4c**; gabazine) analogues were not effective against the AC GABA receptor when tested at 500 μ M (Fig. 4B). This finding is in agreement with a previous finding with **4c** tested at 10 μ M by a patch-clamp technique using AC brain neurons.²⁴ The analogue lacking a 3-substituent (**4a**) demonstrated greater inhibition rather than **4c**. The low activity of **4c** is unexpected when compared with the 3,4-methylenedioxyphenyl (**4d**) and 4-trifluoromethylphenyl (**4e**) analogues, which showed moderate activity. The replacement of the 3-substituent with a 3,4-methylenedioxyphenyl group to give **4d** resulted in a 4-fold increase in inhibition when compared with **4c**. An analogue with a 4-trifluoromethylphenyl group (**4e**) showed 3-fold greater inhibition than **4c**. Among the synthesized compounds, the 4-biphenyl analogue (**4f**) showed the greatest activity, with 92.0% inhibition, an approximately 10-fold increase compared to **4c**. The 4-phenoxyphenyl analogue (**4g**) showed approximately 6-fold enhanced inhibition when compared with **4c**, but decreased inhibition compared with **4f**. The introduction of a 1-naphthyl group to yield **4h** resulted in a drop in inhibition. In contrast, the 2-naphthyl analogue

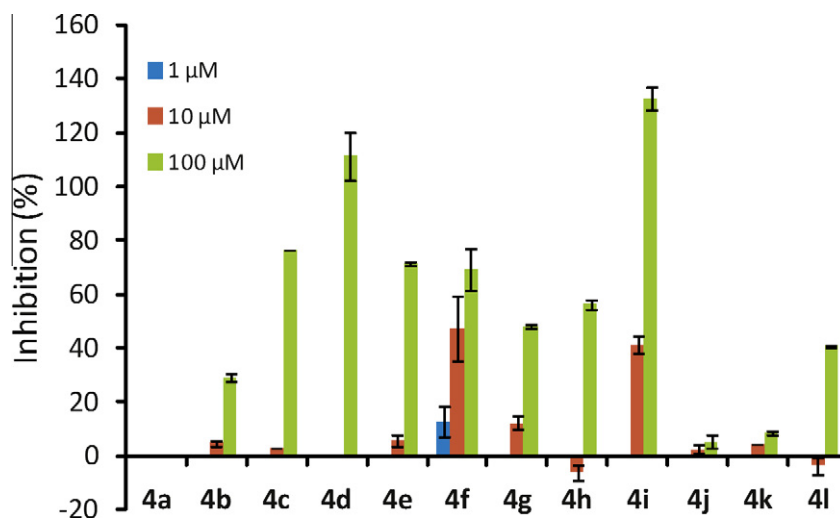


Figure 2. Inhibition of GABA-induced membrane potential changes in SBP GABA receptors. GABA at a concentration corresponding to the EC_{50} (1.0 μ M) was used. Data represent the means of two experiments with bars of the inhibition range, except for the data for 10 and 100 μ M **4f**, which are shown as the means \pm standard deviations of four experiments.

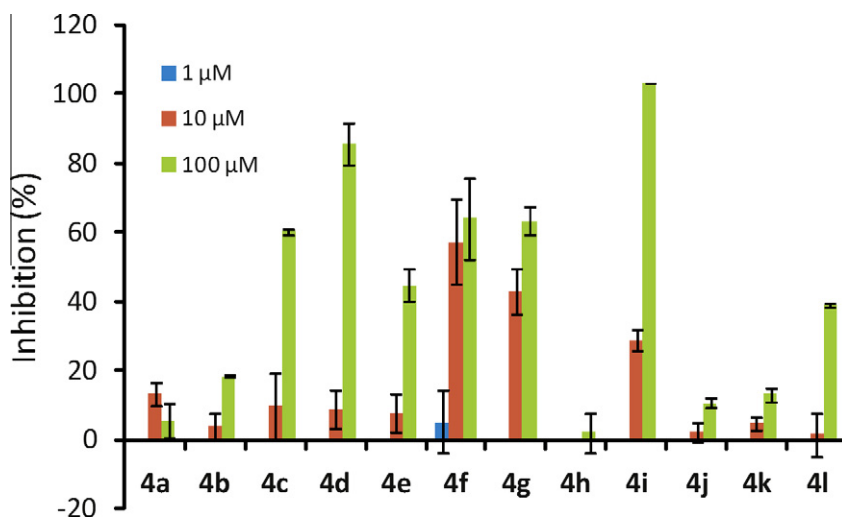


Figure 3. Inhibition of GABA-induced membrane potential changes in CC GABA receptors. GABA at a concentration corresponding to the EC_{50} (2.5 μ M) was used. Data represent the means of two experiments with bars of the inhibition range, except for the data for 10 and 100 μ M **4f**, which are shown as the means \pm standard deviations of four experiments.

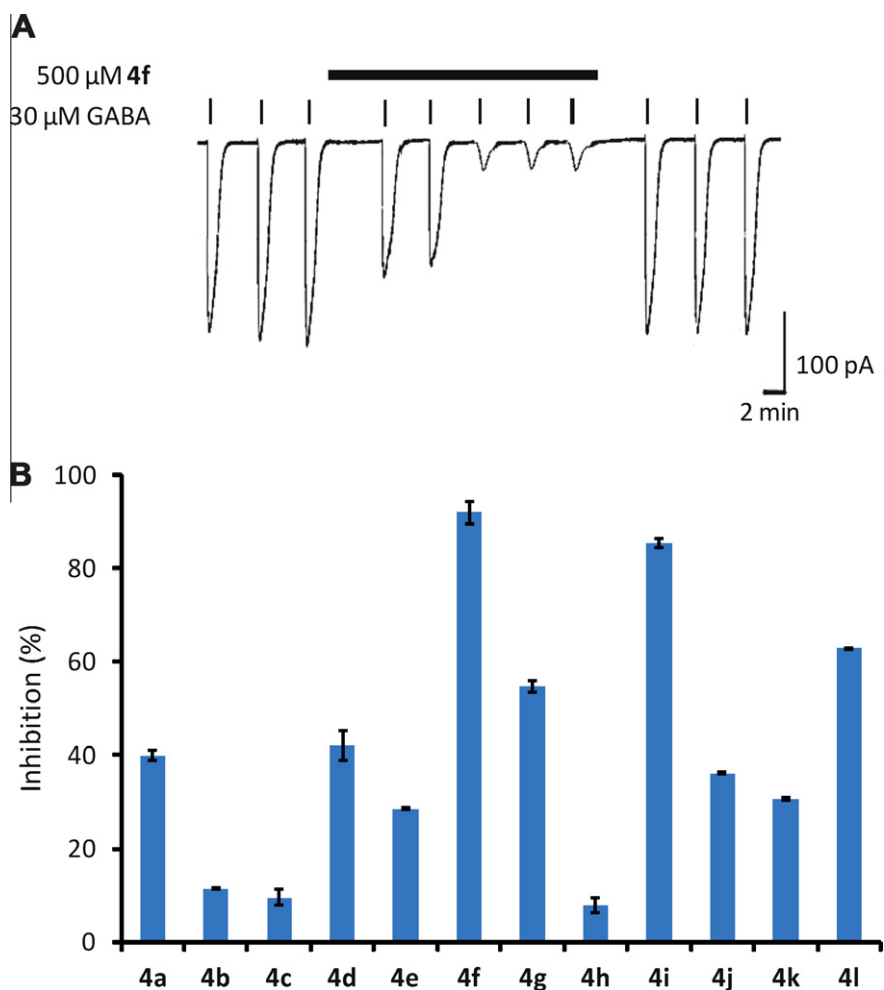


Figure 4. Inhibition of GABA-induced currents in AC GABA receptors. (A) Application protocol represented by current traces of inhibition by 500 μ M **4f**. (B) Inhibition by gabazine and its analogues (500 μ M). GABA at a concentration corresponding to the EC_{50} (30 μ M) was used. Data are the means \pm standard deviations of three or four experiments.

4i) displayed 9-fold greater inhibition than **4c**. The high activity of **4f** and **4i** suggests that long aromatic substituents at the 3-position

of the pyridazine ring are tolerated. The replacement of the 4-methoxyphenyl group of **4c** with 5-membered heteroaromatic

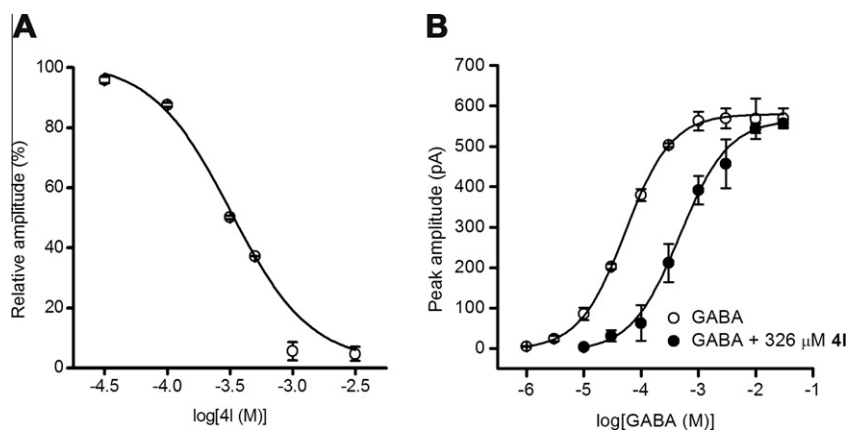


Figure 5. Action of **4l** on AC GABA receptors. The receptors were activated by 30 μM GABA. (A) Concentration-dependent inhibition of GABA-induced currents by **4l**. (B) GABA concentration–response curves in the presence (filled circles) and absence (open circles) of 326 μM **4l**. I_{max} (maximal magnitude of inward currents) = -569 ± 30 pA, $\text{EC}_{50} = 49.2 \pm 10.0$ μM in the absence of **4l**; $I_{\text{max}} = -557 \pm 6$ pA, $\text{EC}_{50} = 496 \pm 64$ μM in the presence of **4l**. Data represent the mean \pm standard deviation of three experiments.

substituents to give **4j**, **4k**, and **4l** increased the inhibition percentage by 3- to 6-fold. The 3-thienyl analogue (**4l**) showed a relatively high activity among analogues with a heteroaromatic 3-substituent, indicating that the lone-pair electrons on the heteroatom of the analogue at this position may provide some favorable electro-negative effects toward receptor interaction. Overall, the inhibition pattern of AC GABA receptors by the analogues differs from that of SBP and CC GABA receptors, suggesting the existence of structural differences in the binding site between insect species.

2.4. Mode of antagonism

To determine whether the synthesized compounds act as competitive antagonists, we examined the GABA concentration–response relationships in the presence and absence of a selected analogue, **4l**, in AC neurons. The IC_{50} value of **4l** was determined to be 346 ± 18 (SD) μM ($n = 3$) from its concentration–response relationships (Fig. 5A). The GABA concentration–response curve in the presence of **4l** showed a parallel rightward shift relative to that in the absence of **4l** (Fig. 5B), indicating that **4l** is a competitive GABA receptor antagonist. Compound **4l** was also examined for antagonism of inhibitory glutamate receptors in AC neurons. This analogue failed to inhibit glutamate-induced currents when tested at 1 and 10 mM (data not shown).

2.5. Homology modeling and ligand docking

The orthosteric binding site in Cys-loop receptors is located at the extracellular interface between the principal and complementary faces of adjacent subunits.²⁵ Loops A–C from the principal face and loops D–F from the complementary face jointly form the GABA binding site. To examine the mechanisms of the interaction of gabazine analogues with insect GABA receptors, we performed ligand docking studies using a homology model. The zwitter ion forms of GABA and the 4-biphenyl analogue (**4f**) were docked into a homology model of the housefly GABA receptor constructed using the X-ray crystal structure of the *Caenorhabditis elegans* glutamate-gated chloride channel as a template.²⁶ We used the housefly GABA receptor for homology modeling in the present study, because the full-length gene encoding the AC GABA receptor has not been cloned and the amino acid sequence of the housefly GABA receptor (GenBank accession AB177547) has a high shared identity (71.1%) with a partial sequence of the AC GABA receptor (GenBank accession FJ612451).

In the docking of GABA into the orthosteric site, which is formed by six loops designated A–F,²⁷ the side chain of Glu202 and the backbone carbonyl oxygen atom of Ser203 in loop B were predicted to function as hydrogen acceptors for the protonated amino group of GABA (Fig. 6A). Arg109 in loop D and Ser174 in loop E serve as hydrogen donors for the carboxylate anion of GABA. Phe204 in loop B and Tyr252 in loop C likely exist near the protonated amino group of GABA (Fig. 6A). These aromatic amino acids may have cation/ π interactions with it, as was recently suggested for the *Drosophila* GABA receptor.²⁸ Amino acids at the equivalent positions are implicated in GABA binding in the GABA_A receptor.²⁹

In the docking of the 4-biphenyl analogue (**4f**) into the orthosteric site, amino acid residues similar to those presumed to be involved in GABA binding were predicted to interact with the carboxyl group and the imino group (Fig. 6B). Hydrogen bonding of the dissociated carboxyl and protonated imino groups of gabazine analogues with neighboring amino acid residues (Arg109, Ser174, Ser203, and Phe204) appeared to play a major role in the binding of gabazine analogues (Fig. 6B). The backbone carbonyl group of Phe204 in loop B was predicted to function as an acceptor for the imino hydrogen atom in place of Glu202, which interacts with GABA. The amino acid of the rat GABA_A receptor $\alpha 1$ subunit that is equivalent to Arg109 has been implicated in interacting with gabazine.³⁰ However, the location of bound gabazine seems to differ from that in our predicted binding pocket.

The docking studies of **4f** predict that its large 3-substituent is tolerable in the potential orthosteric binding site. Our model shows that hydrophobic interactions predominate in the area that accommodates the 3-substituents of the analogues. The phenyl group at one end of the **4f** molecule is likely exposed outside the receptor. Tyr88, Leu90, Tyr107, Val146, Val224, Arg254, Ile245, and Leu247 are predicted to contribute to encompassing the 3-substituent of gabazine analogues. The aromatic 3-substituents may form CH/ π interactions with Val146 in loop A and Leu247 in loop C. In the rat GABA_A and GABA_C receptors, amino acid residues equivalent to Tyr107 and Phe111 in loop D and Phe144 in loop A were reported to contribute to gabazine binding.^{31,32} Tyr107 and Phe144 are found near the **4f** molecule in our docking model, but Phe111 is away from the binding pocket. It is of interest to note that in the rat GABA receptors, gabazine sensitivity depended on whether amino acids at the 107- and 144-positions are phenylalanine or tyrosine and that the three insect GABA receptors used in the present study contain the same amino acids at the 107- and 144-positions as the GABA_C receptor, which has low affinity for

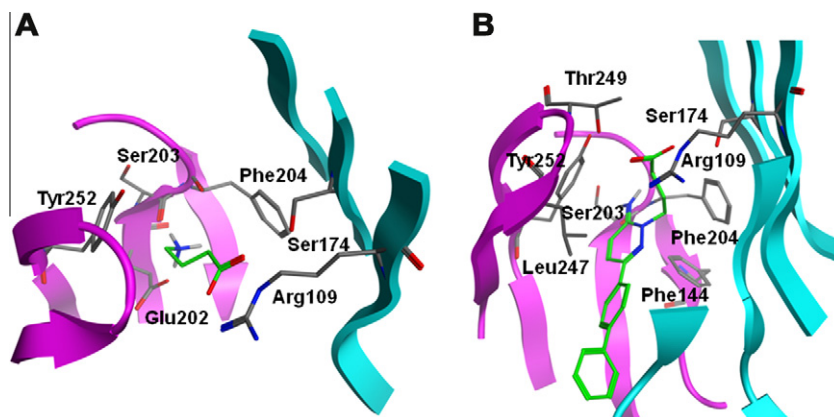


Figure 6. Homology modeling and docking simulation. (A) Docking of GABA into the orthosteric site of a housefly GABA receptor homology model. (B) Docking of **4f**.

gabazine. In addition to Phe144, Val146, a nearby amino acid in loop A, faces the **4f** molecule, which is consistent with the finding that a homologous amino acid lines the GABA binding pocket of the rat receptor.³³ In the model, Val180 in loop F exists at the position where the apex phenyl group of **4f** interacts. This finding is consistent with the finding that this region of loop F in the rat GABA_A receptor was identified as a region lining the GABA binding site.³⁴

In this study, we synthesized gabazine analogues that are more potent than gabazine against insect GABA receptors, but their potency levels are still low compared with the levels reported with GABA_A receptors.³⁰ Analogues with nanomolar affinity for GABA_A receptors and an analogue with low micromolar affinity for GABA_C receptors have recently been reported.^{35,36} Information from ligand docking studies with a homology model using the *C. elegans* glutamate-gated chloride channel X-ray structure as a template proved to be useful for studying the receptor-ligand interaction. Analogues with higher potencies for insect GABA receptors may be obtained by further modification of gabazine.

3. Experimental

3.1. General methods

The melting points of synthesized compounds were determined using a Yanagimoto MP-500D apparatus and are uncorrected. ¹H NMR spectra were recorded on a JEOL JNM-A 400 spectrometer. The chemical shifts (δ values) are given in ppm relative to tetramethylsilane, and the *J* values are given in Hertz. The spin multiplicities are expressed as follows: s (singlet), d (doublet), t (triplet), qn (quintet), and m (multiplet). High resolution mass spectra were obtained with a Waters Synapt G2 spectrometer. Reagents were purchased from Wako Pure Chemical Industries, Ltd. (Osaka, Japan) and Tokyo Chemical Industry Co., Ltd. (Tokyo, Japan), unless otherwise noted.

3.2. General procedure for the synthesis of 3-amino-6-aryl/heteroarylpyridazines (**1b–1i**)

In the case of **1b–1i** and **1l**, a mixture of 3-amino-6-chloropyridazine (388 mg, 3.0 mmol), aryl/heteroarylboronic acid (4.5 mmol), tetrakis(triphenylphosphine)palladium(0) (105 mg), and a 2 M Na₂CO₃ solution (3.3 mL) in toluene (20 mL) was stirred under an argon atmosphere for 30 min at room temperature. In the case of **1j** and **1k**, a mixture of 3-amino-6-chloropyridazine (388 mg, 3.0 mmol), tributyl(heteroaryl)tin (4.1 mmol), and bis(triphenylphosphine)palladium(II) dichloride (198 mg) in THF (10 mL) was stirred under an argon atmosphere for 30 min at room tempera-

ture. In both cases, the reaction mixture was then heated under reflux with stirring under an argon atmosphere until completion of the reaction. After cooling, the reaction mixture was evaporated under reduced pressure to dryness. EtOAc (80 mL) was added to the residue, and the flask containing the suspension was placed in an ultrasonic bath for 5 min. The mixture was filtered, and the filter paper was washed thoroughly with EtOAc (200 mL). The filtrate was evaporated under reduced pressure to dryness. The residue was purified by silica gel column chromatography to yield 3-amino-6-aryl/heteroarylpyridazine (**1b–1i**).

3.3. General procedure for the synthesis of ethyl 4-(6-iminopyridazin-1-yl)butanoates (**3a–3l**)

A mixture of 3-amino-6-aryl/heteroarylpyridazine (**1b–1i**) (1 mmol), ethyl 4-bromobutanoate (292 mg, 1.5 mmol), and *N,N*-dimethylformamide (0.5 mL) was heated at 80 °C for 5 h. After cooling, the precipitate was collected and recrystallized from methanol and diethyl ether to give ethyl 4-(6-imino-3-aryl/heteroarylpyridazin-1-yl)butanoate hydrobromides (**2b–2l**). The hydrobromide (200 mg) was dissolved in a minimal amount of water. A K₂CO₃ solution was used to make the solution alkaline, and then the solution was extracted with a 1:1 mixture of EtOAc and Et₂O. The organic layer was dried with anhydrous Na₂SO₄ and was concentrated under reduced pressure to give ethyl 4-(6-imino-3-aryl/heteroarylpyridazin-1-yl)butanoates (**3b–3l**). Ethyl 4-(6-iminopyridazin-1-yl)butanoate (**3a**) was similarly prepared from 3-amino-6-aryl/heteroarylpyridazine (**1a**).

3.4. General procedure for the synthesis of 4-(6-iminopyridazin-1-yl)butanoic acid hydrochlorides (**4a–4l**)

A solution of ethyl 4-(6-imino-3-aryl/heteroarylpyridazin-1-yl)butanoate (**3b–3l**) (0.5 mmol) in glacial acetic acid (10 mL) and concentrated HCl (3 mL) was heated at 100 °C for approximately 12 h. After cooling, the reaction mixture was evaporated to dryness under reduced pressure. The residue was recrystallized with AcOH and EtOAc to afford 4-(6-imino-3-aryl/heteroarylpyridazin-1-yl)butanoic acid hydrochlorides (**4b–4l**). 4-(6-iminopyridazin-1-yl)butanoic acid hydrochloride (**4a**) was similarly obtained from ethyl 4-(6-iminopyridazin-1-yl)butanoate (**3a**).

3.4.1. 4-(6-Iminopyridazin-1-yl)butanoic acid hydrochloride (**4a**)

Yield 8% (from **1a**), mp 144–145 °C. ¹H NMR (CD₃OD) δ 2.15 (tt, 2H, *J* = 7.3, 6.8 Hz, –CO–CH₂–CH₂–CH₂–), 2.50 (t, 2H, *J* = 6.8 Hz, –CO–CH₂–CH₂–CH₂–), 4.37 (t, 2H, *J* = 7.3 Hz, –CO–CH₂–CH₂–CH₂–),

7.55 (dd, 1H, $J = 9.4, 1.5$ Hz, H-3), 7.73 (dd, 1H, $J = 9.4, 4.2$ Hz, H-4), 8.39 (dd, 1H, $J = 4.2, 1.5$ Hz, H-5). HRMS Calcd for $C_8H_{12}N_3O_2$ [$M^+ - Cl$] 182.0930. Found 182.0919.

3.4.2. 4-[6-Imino-3-phenylpyridazin-1-yl]butanoic acid hydrochloride (4b)

Yield 11% (for three steps), mp 265–267 °C (dec). 1H NMR (CD_3OD) δ 2.23 (tt, 2H, $J = 7.3, 6.8$ Hz, $-CO-CH_2-CH_2-CH_2-$), 2.56 (t, 2H, $J = 6.8$ Hz, $-CO-CH_2-CH_2-CH_2-$), 4.46 (t, 2H, $J = 7.3$ Hz, $-CO-CH_2-CH_2-CH_2-$), 7.53–7.56 (m, 3H, H-3', H-4'), 7.64 (d, 1H, $J = 9.6$ Hz, H-5), 7.98–8.00 (m, 2H, H-2'), 8.32 (d, 1H, $J = 9.6$ Hz, H-4). HRMS Calcd for $C_{14}H_{16}N_3O_2$ [$M^+ - Cl$] 258.1243. Found 258.1235.

3.4.3. 4-[6-Imino-3-(4-methoxyphenyl)pyridazin-1-yl]butanoic acid hydrochloride (4c) (Gabazine)

Yield 18% (for three steps), mp 199–201 °C; 1H NMR (CD_3OD) δ 2.22 (tt, 2H, $J = 7.1, 6.9$ Hz, $-CO-CH_2-CH_2-CH_2-$), 2.55 (t, 2H, $J = 6.9$ Hz, $-CO-CH_2-CH_2-CH_2-$), 3.87 (s, 3H, $-O-CH_3$), 4.43 (t, 2H, $J = 7.1$ Hz, $-CO-CH_2-CH_2-CH_2-$), 7.07 (dd, 2H, $J = 6.9, 2.0$ Hz, H-3'), 7.59 (d, 1H, $J = 9.6$ Hz, H-5), 7.95 (dd, 2H, $J = 6.9, 2.0$ Hz, H-2'), 8.28 (d, 1H, $J = 9.6$ Hz, H-4). HRMS Calcd for $C_{15}H_{18}N_3O_3$ [$M^+ - Cl$] 288.1348. Found 288.1329.

3.4.4. 4-[6-Imino-3-(3,4-methylenedioxyphenyl)pyridazin-1-yl]butanoic acid hydrochloride (4d)

Yield 19% (for three steps), mp 214–215 °C. 1H NMR (CD_3OD) δ 2.21 (tt, 2H, $J = 7.3$ Hz, 6.8 Hz, $-CO-CH_2-CH_2-CH_2-$), 2.55 (t, 2H, $J = 6.8$ Hz, $-CO-CH_2-CH_2-CH_2-$), 4.42 (t, 2H, $J = 7.3$ Hz, $-CO-CH_2-CH_2-CH_2-$), 6.06 (s, 2H, $-O-CH_2-O-$), 6.97 (m, 1H, H-6'), 7.51–7.53 (m, 2H, H-2', H-5'), 7.57 (d, 1H, $J = 9.8$ Hz, H-5), 8.25 (d, 1H, $J = 9.8$ Hz, H-4). HRMS Calcd for $C_{15}H_{16}N_3O_4$ [$M^+ - Cl$] 302.1141. Found 302.1142.

3.4.5. 4-[6-Imino-3-(4-trifluoromethylphenyl)pyridazin-1-yl]butanoic acid hydrochloride (4e)

Yield 17% (for three steps), mp 257–260 °C (dec). 1H NMR (CD_3OD) δ 2.25 (tt, 2H, $J = 7.1, 6.9$ Hz, $-CO-CH_2-CH_2-CH_2-$), 2.57 (t, 2H, $J = 6.9$ Hz, $-CO-CH_2-CH_2-CH_2-$), 4.49 (t, 2H, $J = 7.1$ Hz, $-CO-CH_2-CH_2-CH_2-$), 7.68 (d, 1H, $J = 9.7$ Hz, H-5), 7.86 (dd, 2H, $J = 8.8, 0.6$ Hz, H-2'), 8.19 (dd, 2H, $J = 8.8, 0.6$ Hz, H-3'), 8.38 (d, 1H, $J = 9.7$ Hz, H-4). HRMS Calcd for $C_{15}H_{15}F_3N_3O_2$ [$M^+ - Cl$] 326.1116. Found 326.1102.

3.4.6. 4-[3-(4-Biphenyl)-6-iminopyridazin-1-yl]butanoic acid hydrochloride (4f)

Yield 21% (for three steps), mp 234–236 °C. 1H NMR (CD_3OD) δ 2.24 (qn, 2H, $J = 6.8$ Hz, $-CO-CH_2-CH_2-CH_2-$), 2.57 (t, 2H, $J = 6.8$ Hz, $-CO-CH_2-CH_2-CH_2-$), 4.47 (t, 2H, $J = 6.8$ Hz, $-CO-CH_2-CH_2-CH_2-$), 7.39 (t, 1H, $J = 6.8$ Hz, H-4''), 7.47–7.50 (m, 2H, H-3''), 7.64 (d, 1H, $J = 9.6$ Hz, H-5), 7.68–7.71 (m, 2H, H-2''), 7.81 (dd, 2H, $J = 6.8, 2.0$ Hz, H-2'), 8.08 (dd, 2H, $J = 6.8, 2.0$ Hz, H-3'), 8.37 (d, 1H, $J = 9.6$ Hz, H-4). HRMS Calcd for $C_{20}H_{20}N_3O_2$ [$M^+ - Cl$] 334.1556. Found 334.1537.

3.4.7. 4-[6-Imino-3-(4-phenoxyphenyl)pyridazin-1-yl]butanoic acid hydrochloride (4g)

Yield 50% (for three steps), mp 208–210 °C. 1H NMR (CD_3OD) δ 2.22 (tt, 2H, $J = 7.3, 6.8$ Hz, $-CO-CH_2-CH_2-CH_2-$), 2.55 (t, 2H, $J = 6.8$ Hz, $-CO-CH_2-CH_2-CH_2-$), 4.44 (t, 2H, $J = 7.3$ Hz, $-CO-CH_2-CH_2-CH_2-$), 7.06–7.10 (m, 4H, H-2'', H-3''), 7.18–7.22 (m, 1H, H-4''), 7.39–7.44 (m, 2H, H-2'), 7.61 (d, 1H, $J = 9.6$ Hz, H-5), 7.98–8.00 (m, 2H, H-3'), 8.30 (d, 1H, $J = 9.6$ Hz, H-4). HRMS Calcd for $C_{20}H_{20}N_3O_3$ [$M^+ - Cl$] 350.1505. Found 350.1479.

3.4.8. 4-[6-Imino-3-(1-naphthyl)pyridazin-1-yl]butanoic acid hydrochloride (4h)

Yield 23% (for three steps), mp 219–221 °C. 1H NMR (CD_3OD) δ 2.25 (tt, 2H, $J = 7.3, 6.8$ Hz, $-CO-CH_2-CH_2-CH_2-$), 2.57 (t, 2H, $J = 6.8$ Hz, $-CO-CH_2-CH_2-CH_2-$), 4.47 (t, 2H, $J = 7.3$ Hz, $-CO-CH_2-CH_2-CH_2-$), 7.56–7.64 (m, 3H, H-5, H-4', H-5'), 7.67–7.70 (m, 2H, H-3', H-6'), 8.00–8.08 (m, 4H, H-4, H-2', H-7', H-8'). HRMS Calcd for $C_{18}H_{18}N_3O_2$ [$M^+ - Cl$] 308.1399. Found 308.1405.

3.4.9. 4-[6-Imino-3-(2-naphthyl)pyridazin-1-yl]butanoic acid hydrochloride (4i)

Yield 5% (for three steps), mp 225–227 °C. 1H NMR (CD_3OD) δ 2.26 (qn, 2H, $J = 6.8$ Hz, $-CO-CH_2-CH_2-CH_2-$), 2.59 (t, 2H, $J = 6.8$ Hz, $-CO-CH_2-CH_2-CH_2-$), 4.49 (t, 2H, $J = 6.8$ Hz, $-CO-CH_2-CH_2-CH_2-$), 7.57–7.62 (m, 2H, H-6', H-7'), 7.66 (d, 1H, $J = 9.8$ Hz, H-5), 7.93–7.95 (m, 1H, H-3'), 8.02 (d, 2H, $J = 8.8$ Hz, H-5', H-8'), 8.12 (dd, 1H, $J = 8.8, 2.0$ Hz, H-4'), 8.50 (d, 2H, $J = 9.8$ Hz, H-4, H-1'). HRMS Calcd for $C_{18}H_{18}N_3O_2$ [$M^+ - Cl$] 308.1399. Found 308.1405.

3.4.10. 4-[3-(2-Furyl)-6-iminopyridazin-1-yl]butanoic acid hydrochloride (4j)

Yield 34% (for three steps), mp 230–232 °C (dec). 1H NMR (CD_3OD) δ 2.19 (tt, 2H, $J = 7.1, 6.8$ Hz, $-CO-CH_2-CH_2-CH_2-$), 2.54 (t, 2H, $J = 6.8$ Hz, $-CO-CH_2-CH_2-CH_2-$), 4.39 (t, 2H, $J = 7.1$ Hz, $-CO-CH_2-CH_2-CH_2-$), 6.68 (dd, 1H, $J = 3.8, 1.8$ Hz, H-4'), 7.24 (dd, 1H, $J = 3.8, 0.8$ Hz, H-5'), 7.59 (d, 1H, $J = 9.6$ Hz, H-5), 7.79 (dd, 1H, $J = 1.8, 0.8$ Hz, H-3'), 8.15 (d, 1H, $J = 9.6$ Hz, H-4). HRMS Calcd for $C_{12}H_{14}N_3O_3$ [$M^+ - Cl$] 248.1035. Found 248.1041.

3.4.11. 4-[6-Imino-3-(2-thienyl)pyridazin-1-yl]butanoic acid hydrochloride (4k)

Yield 23% (for three steps), mp 225–227 °C. 1H NMR (CD_3OD) δ 2.20 (tt, 2H, $J = 7.1, 6.8$ Hz, $-CO-CH_2-CH_2-CH_2-$), 2.55 (t, 2H, $J = 6.8$ Hz, $-CO-CH_2-CH_2-CH_2-$), 4.37 (t, 2H, $J = 7.1$ Hz, $-CO-CH_2-CH_2-CH_2-$), 7.20 (dd, 1H, $J = 5.2, 3.7$ Hz, H-4'), 7.57 (d, 1H, $J = 9.6$ Hz, H-5), 7.68 (dd, 1H, $J = 5.2, 1.3$ Hz, H-5'), 7.81 (dd, 1H, $J = 3.7, 1.3$ Hz, H-3'), 8.27 (d, 1H, $J = 9.6$ Hz, H-4). HRMS Calcd for $C_{12}H_{14}N_3O_2S$ [$M^+ - Cl$] 264.0807. Found 264.0802.

3.4.12. 4-[6-Imino-3-(3-thienyl)pyridazin-1-yl]butanoic acid hydrochloride (4l)

Yield 21% (for three steps), mp 215–217 °C. 1H NMR (CD_3OD) δ 2.21 (tt, 2H, $J = 7.1, 6.8$ Hz, $-CO-CH_2-CH_2-CH_2-$), 2.54 (t, 2H, $J = 6.8$ Hz, $-CO-CH_2-CH_2-CH_2-$), 4.41 (t, 2H, $J = 7.1$ Hz, $-CO-CH_2-CH_2-CH_2-$), 7.57–7.61 (m, 2H, H-5, H-5'), 7.70 (dd, 1H, $J = 5.2, 1.5$ Hz, H-4'), 8.19–8.20 (m, 1H, H-2'), 8.27 (d, 1H, $J = 9.3$ Hz, H-4). HRMS Calcd for $C_{12}H_{14}N_3O_2S$ [$M^+ - Cl$] 264.0807. Found 264.0802.

3.5. FMP assays

A *Drosophila* S2 cell line expressing GABA receptors from SBPs (*Laodelphax striatella* [*striatellus*] (Fallén)) (GenBank accession AB253526.1) or CCs (*Spodoptera litura* (Fabricius)) (GenBank DD171257.1) was used in this assay. These stable cell lines were generated as previously reported.¹⁸ The cells were washed and dispersed in a saline buffer (120 mM NaCl, 5 mM KCl, 2 mM $CaCl_2$, 8 mM $MgCl_2$, 10 mM HEPES, and 32 mM sucrose, adjusted to pH 7.2 with an NaOH solution), and aliquots (100 μ L each) of this cell suspension (5×10^5 cells) were added to 96-well microplates for the fluorescent assay. After 10 min, the cells were spun down at 1400 rpm for 5 min and loaded with the FMP blue dye (Molecular Devices; 100 μ L) at room temperature for 20 min. Gabazine and gabazine analogues were first dissolved in DMSO and diluted with a saline buffer. Gabazine or a gabazine analogue in a saline buffer (25 μ L) containing 1% DMSO was added to the cells in each well and incubated with for 74 s. Subsequently, GABA in a saline buffer

(25 μL) was added to each well. GABA concentrations corresponding to the EC_{50} s for SBP and CC receptors (1.0 and 2.5 μM , respectively) were used for receptor activation. The fluorescent intensity at 560 nm, upon excitation at 530 nm, was monitored using a FlexStation II plate reader (Molecular Devices). The inhibition percentage was determined based on changes in fluorescence before (the average value for 20 s) and after (the maximal value after 10–60 s) the addition of GABA. Each assay was repeated twice, unless otherwise noted.

3.6. Electrophysiology

3.6.1. Isolation of neurons from ACs

The sixth abdominal ganglia were dissected from adult male ACs (*Periplaneta americana* (Linnaeus)) and were placed in Ca^{2+} -free saline containing 200 mM NaCl, 3.1 mM KCl, 4 mM MgCl_2 , 20 mM D-glucose, and 10 mM HEPES, adjusted to pH 7.4 with an NaOH solution. The ganglia were incubated for 20 min at 25 °C in Ca^{2+} -free saline containing collagenase (0.5 mg mL^{-1}) and trypsin (0.2 mg mL^{-1}) and were rinsed with Ca^{2+} -free saline twice. The ganglia were then placed in Ca^{2+} -containing saline (200 mM NaCl, 3.1 mM KCl, 4 mM MgCl_2 , 5 mM CaCl_2 , 20 mM D-glucose, and 10 mM HEPES-acid, adjusted to pH 7.4 with NaOH) supplemented with 10% fetal bovine serum (Invitrogen). The neurons were dissociated using a pipette tip. The dissociated neurons were kept on coverslips coated with poly-D-lysine solution (1 mg mL^{-1} , Sigma-Aldrich) for 45 min. The neurons were incubated at 25 °C for 16 h before whole-cell current recordings.

3.6.2. Whole-cell patch-clamp analysis

Membrane currents were recorded with the whole-cell recording arrangement using a patch-clamp amplifier (EPC-8; HEKA) at 20 °C. The AC neurons were perfused continuously with an external solution containing 200 mM NaCl, 3.1 mM KCl, 4 mM MgCl_2 , 5 mM CaCl_2 , 25 mM D-glucose, and 10 mM HEPES-acid, adjusted to pH 7.4 with NaOH (405 mOsm L^{-1}). The recording electrodes had a resistance of 3–5 $\text{M}\Omega$ when filled with the pipette solution containing 15 mM NaCl, 170 mM KCl, 1 mM MgCl_2 , 0.5 mM CaCl_2 , 10 mM EGTA, 10 mM HEPES, and 5 mM ATP, adjusted to pH 7.4 with NaOH (405 mOsm L^{-1}). GABA, gabazine, and its analogues were dissolved in the external solution. The external solution surrounding the cells was completely changed with a solution containing GABA or antagonists within 2 s. Sixth abdominal ganglion neurons were incubated for 2 min in a cockroach saline solution followed by the 2–3-s application of 30 μM GABA (a concentration corresponding to the EC_{50} for AC receptors). GABA-induced currents were measured at a holding potential of -60 mV. This process was repeated 2 or 3 times to confirm the constant amplitude of GABA-induced currents. After this process, the neurons were perfused with a bath solution containing gabazine or a gabazine analogue for 5 min, and during the perfusion, GABA was repeatedly applied 5 times to obtain the highest and constant inhibition. Finally, GABA was applied to confirm the integrity of the cell. Each assay was repeated three or four times.

3.7. Molecular modeling and ligand docking studies

The homology model of the housefly (*Musca domestica* (Linnaeus)) GABA receptor was generated using the X-ray crystal structure of the *C. elegans* glutamate-gated chloride channel (PDB: 3RIF) as a template.²⁶ MOE 2010.10 software (Chemical Computing Group) was used to create the model. The sequence of the housefly GABA subunit (accession No. AB177547) was retrieved from GenBank. The alignment of the two protein sequences was carried out using ClustalW software. Geometry optimization was performed using the AMBER99 force field. The structures of the zwitter ion

forms of GABA and **4f** used in the docking studies were created using the Molecule Builder of MOE. Compound **4f** was docked as a protonated imino form, although it exists as resonance forms.³⁷ The created ligands were docked into the potential binding site of the generated model using ASEDock 2011.01.27 software (Chemical Computing Group). The energy of the receptor and ligands was minimized using the MMFF94x force field. The potential docking site was searched using the Site Finder of MOE. The stable conformations of ligands were obtained by the conformational search. Tether weight was added to all receptor backbone atoms within 4.5 Å from a ligand, while others were free. The binding mode with the highest score was chosen for the final representation.

Acknowledgments

We thank Dr. T. Nakao (Mitsui Chemicals Agro, Inc.) for critical reading of this manuscript. This work was supported in part by KAKENHI (a Grant-in-Aid for Scientific Research) (C).

References and notes

- Hevers, W.; Lüddens, H. *Mol. Neurobiol.* **1998**, *18*, 35.
- Bettler, B.; Kaupmann, K.; Mosbacher, J.; Gassmann, M. *Physiol. Rev.* **2004**, *84*, 835.
- Sine, S. M.; Engel, A. G. *Nature* **2006**, *440*, 448.
- Whiting, P. J.; Bonnert, T. P.; McKernan, R. M.; Farrar, S.; Le Bourdellès, B.; Heavens, R. P.; Smith, D. W.; Hewson, L.; Rigby, M. R.; Sirinathsinghji, D. J. S.; Thompson, S. A.; Wafford, K. A. *Ann. N.Y. Acad. Sci.* **1999**, *868*, 645.
- Johnston, G. A. R. *Pharmacol. Ther.* **1996**, *69*, 173.
- Krishek, B. J.; Moss, S. J.; Smart, T. G. *Neuropharmacology* **1996**, *35*, 1289.
- Buckingham, S. D.; Sattelle, D. B. In Gilbert, L. I., Iatrou, K., Gill, S. S., Eds.; *Comprehensive Molecular Insect Science*; Elsevier Pergamon: Amsterdam, 2004; Vol. 5, pp. 107–142.
- French-Constant, R. H.; Rocheleau, T. A.; Steichen, J. C.; Chalmers, A. E. *Nature* **1993**, *363*, 449.
- Mezler, M.; Müller, T.; Raming, K. *Eur. J. Neurosci.* **2001**, *13*, 477.
- Gisselmann, G.; Plonka, J.; Pusch, H.; Hatt, H. *Br. J. Pharmacol.* **2004**, *142*, 409.
- Buckingham, S. D.; Biggin, P. C.; Sattelle, B. M.; Brown, L. A.; Sattelle, D. B. *Mol. Pharmacol.* **2005**, *68*, 942.
- Ozoe, Y.; Takeda, M.; Matsuda, K. In *Inshaaya, I., Horowitz, A. R., Eds.; Biorational Control of Arthropod Pests*; Springer: Heidelberg, 2009; pp 131–162.
- Raymond-Delpech, V.; Matsuda, K.; Sattelle, B. M.; Rauh, J. J.; Sattelle, D. B. *Invert. Neurosci.* **2005**, *5*, 119.
- Ueno, S.; Bracamontes, J.; Zorumski, C.; Weiss, D. S.; Steinbach, J. H. *J. Neurosci.* **1997**, *17*, 625.
- Chambon, J.-P.; Feltz, P.; Heaulme, M.; Restle, S.; Schlichter, R.; Biziere, K.; Wermuth, C. G. *Proc. Natl. Acad. Sci. U.S.A.* **1985**, *82*, 1832.
- Hosie, A. M.; Sattelle, D. B. *Br. J. Pharmacol.* **1996**, *119*, 1577.
- Satoh, H.; Daido, H.; Nakamura, T. *Neurosci. Lett.* **2005**, *381*, 125.
- Narusuye, K.; Nakao, T.; Abe, R.; Nagatomi, Y.; Hirase, K.; Ozoe, Y. *Insect Mol. Biol.* **2007**, *16*, 723.
- Wermuth, C.-G.; Bourguignon, J.-J.; Schlewer, G.; Gies, J.-P.; Schoenfelder, A.; Melikian, A.; Bouchet, M.-J.; Chantreux, D.; Molimard, J.-C.; Heaulme, M.; Chambon, J.-P.; Biziere, K. *J. Med. Chem.* **1987**, *30*, 239.
- Melikian, A.; Schlewer, G.; Chambon, J.-P.; Wermuth, C. G. *J. Med. Chem.* **1992**, *35*, 4092.
- Gavande, N.; Johnston, G. A. R.; Hanrahan, J. R.; Chebib, M. *Org. Biomol. Chem.* **2010**, *8*, 4131.
- Schroeder, K. S.; Neagle, B. D. *J. Biomol. Screen.* **1996**, *1*, 75.
- Joesch, C.; Guevarra, E.; Parel, S. P.; Bergner, A.; Zbinden, P.; Konrad, D.; Albrecht, H. J. *Biomol. Screen.* **2008**, *13*, 218.
- Aydar, E.; Beadle, D. J. *J. Insect Physiol.* **1999**, *45*, 213.
- Miller, P. S.; Smart, T. G. *Trends Pharmacol. Sci.* **2010**, *31*, 161.
- Hibbs, R. E.; Gouaux, E. *Nature* **2011**, *474*, 54.
- Sander, T.; Frølund, B.; Bruun, A. T.; Ivanov, I.; McCammon, J. A.; Balle, T. *Proteins* **2011**, *79*, 1458.
- Lumms, S. C. R.; McGonigle, I.; Ashby, J. A.; Dougherty, D. A. *J. Neurosci.* **2011**, *31*, 12371.
- Amin, J.; Weiss, D. S. *Nature* **1993**, *366*, 565.
- Holden, J. H.; Czajkowski, C. J. *Biol. Chem.* **2002**, *277*, 18785.
- Sigel, E.; Baur, R.; Kellenberger, S.; Malherbe, P. *EMBO J.* **1992**, *11*, 2017.
- Zhang, J.; Xue, F.; Chang, Y. *Mol. Pharmacol.* **2008**, *74*, 941.
- Boileau, A. J.; Newell, J. G.; Czajkowski, C. J. *Biol. Chem.* **2002**, *277*, 2931.
- Newell, J. G.; Czajkowski, C. J. *Biol. Chem.* **2003**, *278*, 13166.
- Iqbal, F.; Ellwood, R.; Mortensen, M.; Smart, T. G.; Baker, J. R. *Bioorg. Med. Chem. Lett.* **2011**, *21*, 4252.
- Yamamoto, I.; Carland, J. E.; Locock, K.; Gavande, N.; Absalom, N.; Hanrahan, J. R.; Allan, R. D.; Johnston, G. A. R.; Chebib, M. *ACS Chem. Neurosci.* **2012**, *3*, 293.
- Van der Brempt, C.; Evrard, G.; Durant, F. *Acta Cryst.* **1986**, *C42*, 1206.